

## **A comprehensive analysis and rational designing of efficient Fe-based oxygen electrocatalysts for metal-air batteries**

R. Nandan,<sup>a</sup> A. Gautam,<sup>a</sup> S. Tripathi<sup>a</sup> and K. K. Nanda<sup>a,\*</sup>

<sup>a</sup>Materials Research Centre,

Indian institute of Science,

Bangalore-560012, India.

\*E-mail: [nanda@iisc.ac.in](mailto:nanda@iisc.ac.in)

Fax: +91-80-2360 7316; Ph:+91-80-2293 2996

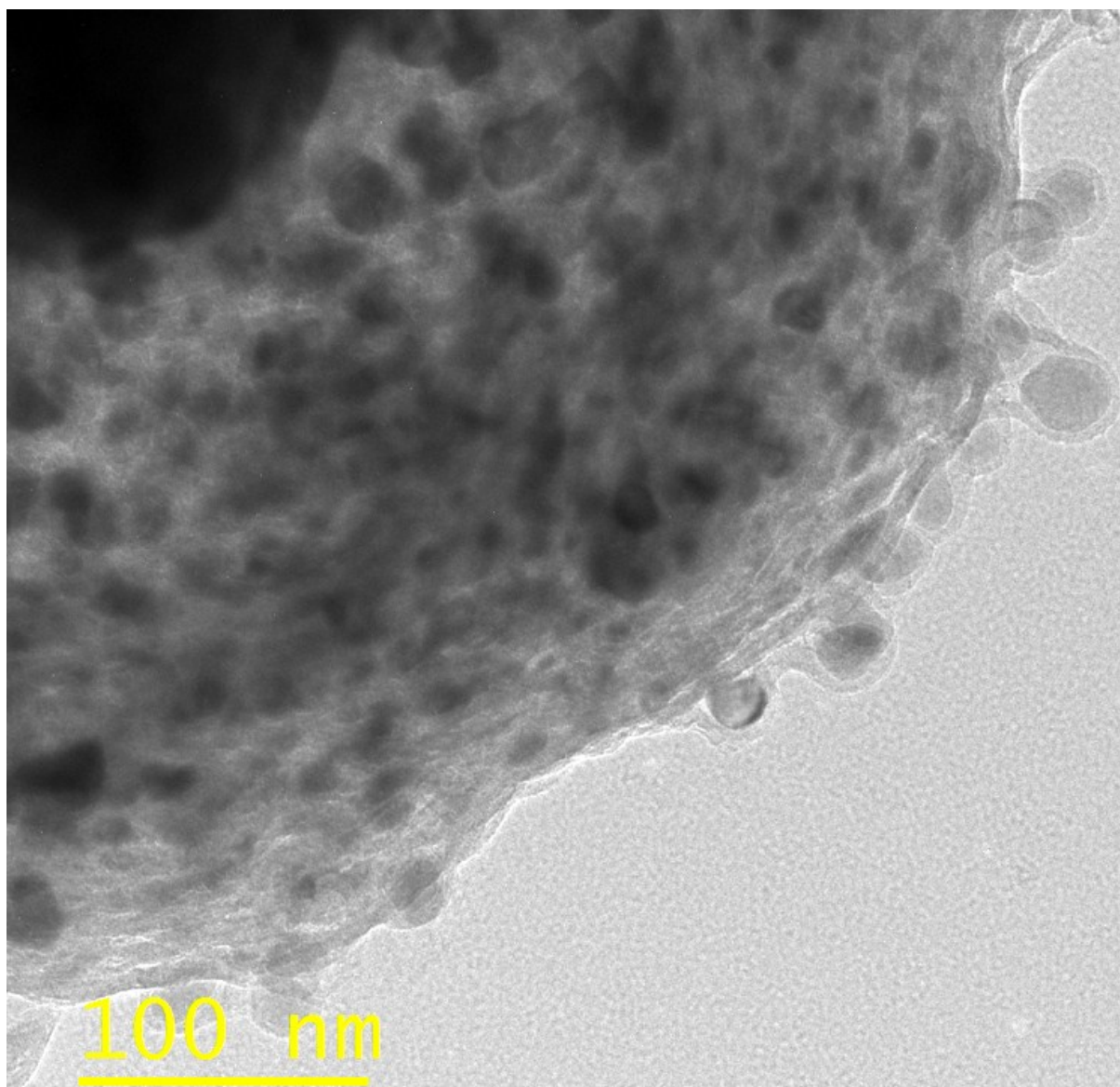


**Figure S1.** TEM image of Fe-Fe<sub>3</sub>C enriched carbon sphere (FC3R).

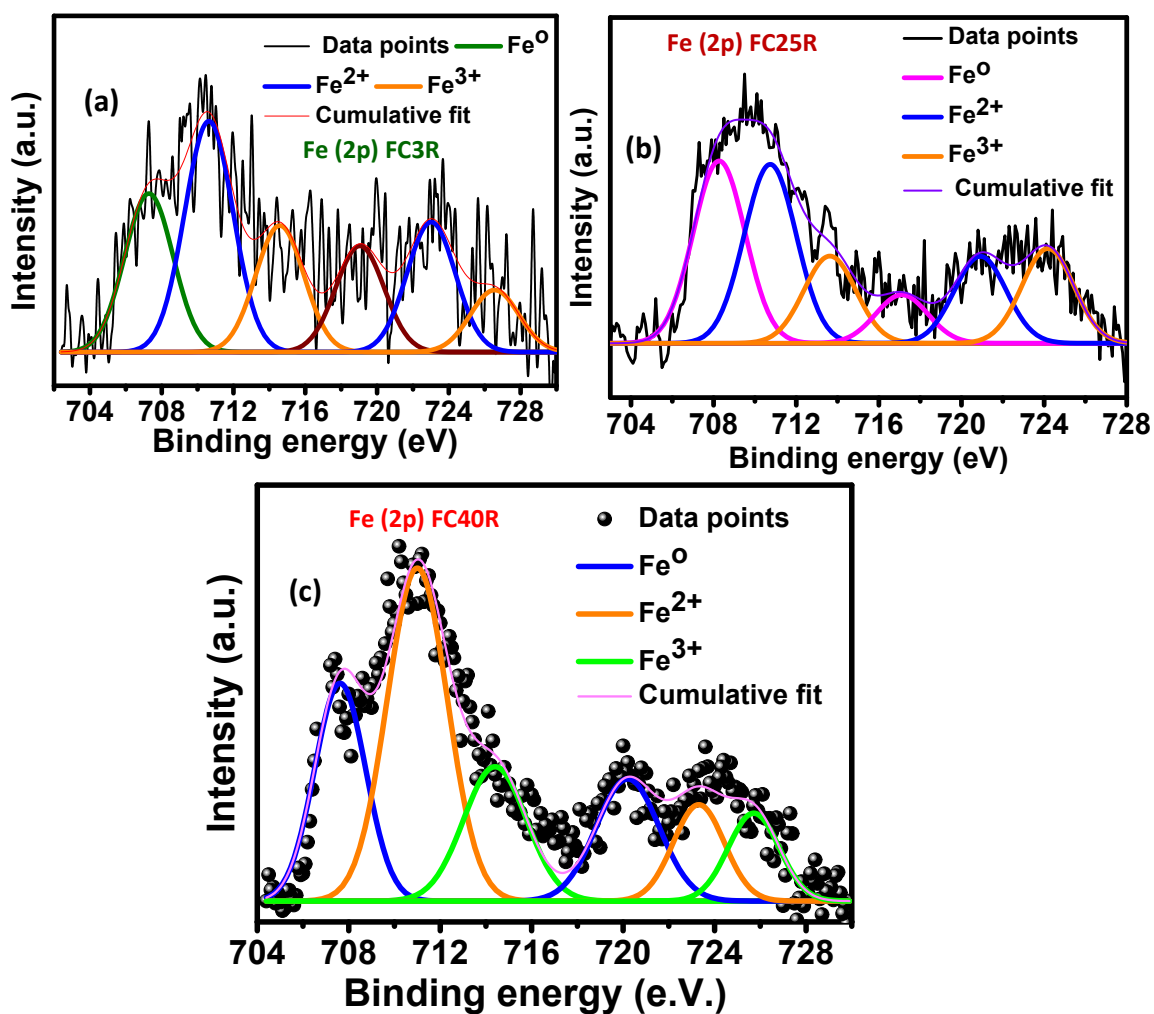


**Figure S2.** (a-c) Deconvoluted Fe (2p) core spectra of FC3R, FC25R and FC40R, respectively

The deconvolution of Fe2p core spectrum of FC3R (fig. S2a) reveals several peaks centred around 708 and 719 eV that can be attributed to  $2p_{3/2}$  and  $2p_{1/2}$  metallic iron ( $\text{Fe}^0$ ). Similarly, the peaks centred around 710.5, 714 and 722, 725 eV can be attributed to the  $2p_{3/2}$  and  $2p_{1/2}$ , of  $\text{Fe}^{2+}$ ,  $\text{Fe}^{3+}$ , respectively.

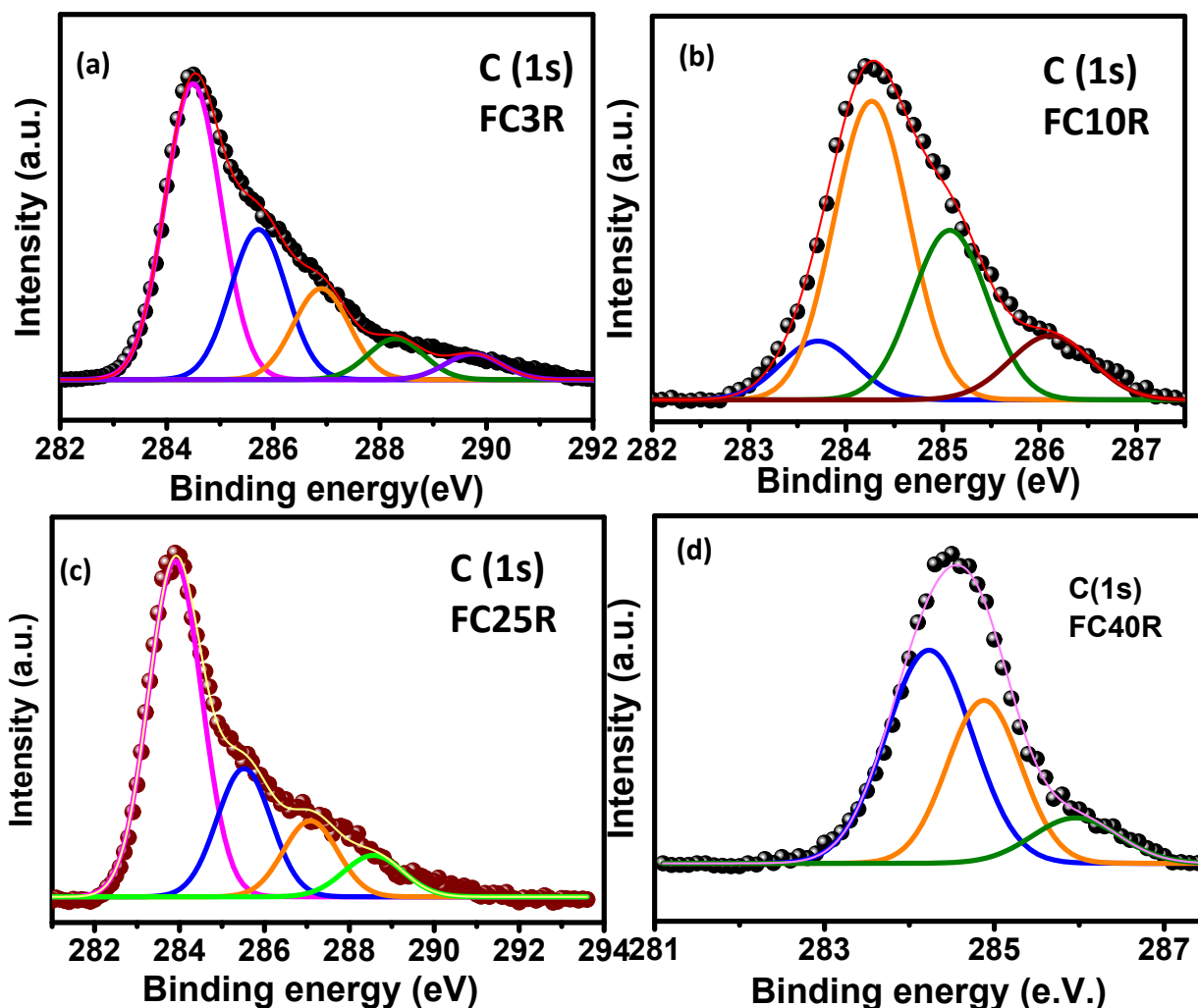


**Figure S3.** (a-d) Deconvoluted core C 1s spectra of FC3R, FC10R, FC25R and FC40R.

The deconvoluted C1s core spectrum of FC3R reveals several peaks centred around 284.5, 285.7, 286.9, 288.3 and 289.7 eV that correspond to  $sp^2$  carbon,  $sp^2$  carbon-nitrogen,  $sp^3$  carbon-nitrogen and the other two peaks can be assigned to carbon-oxygen interactions, respectively.<sup>1-3</sup> Similarly in FC10R, the peaks centred around 283.7, 284.3, 285.1 and 286.1 eV can be assigned to the Fe-C interaction,  $sp^2$  carbon,  $sp^2$  carbon-nitrogen and  $sp^3$  carbon-nitrogen species. The peaks centred around 284.1, 286.3, 288 and 290 eV correspond to  $sp^2$  carbon,  $sp^2$  carbon-nitrogen and  $sp^3$  carbon-nitrogen species in FC25R. Likewise, the peaks concentrated around 284.2, 284.9 and 285.9 eV can be assigned to the  $sp^2$  carbon,  $sp^2$  carbon-nitrogen and  $sp^3$  carbon species in the FC40R.<sup>1-3</sup>

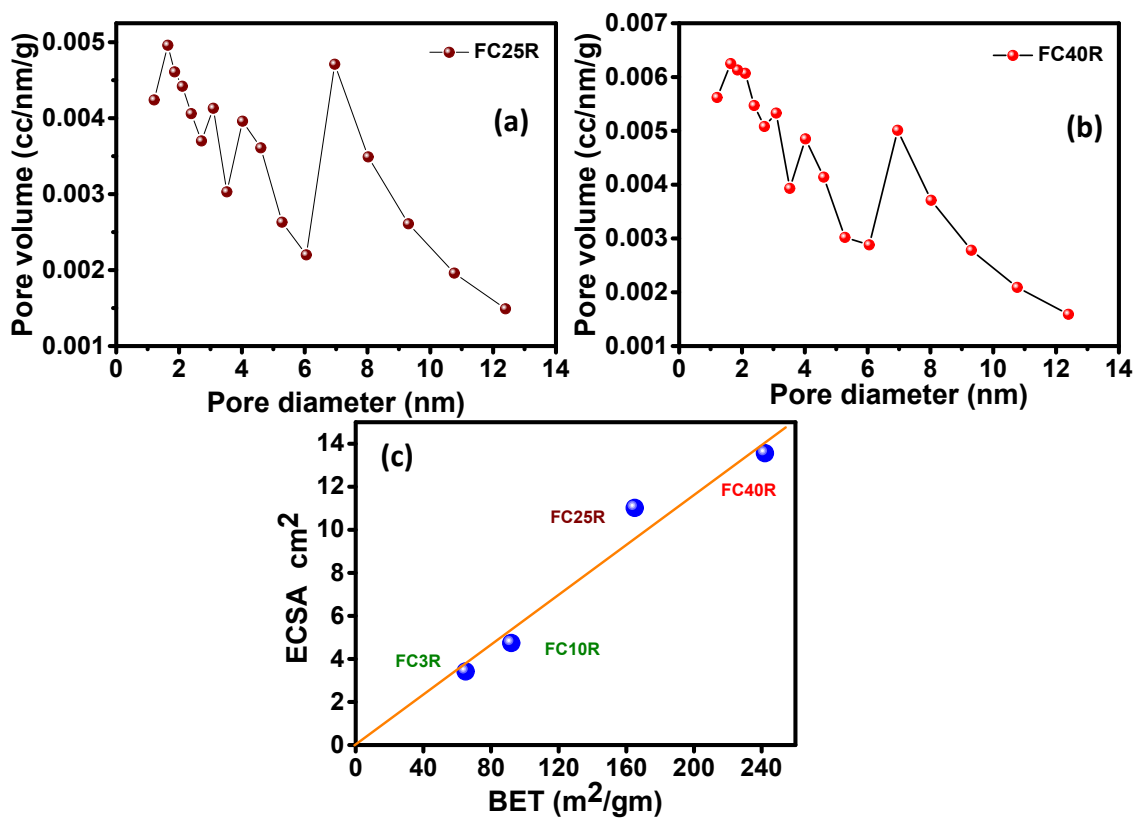


**Figure S4.** (a,b) pore size distribution in FC25R and FC40R. (c) Correlation between ECSA and BET surface area for FCMR (M= 3, 10, 25 and 40). The solid line is the guide for eye. The linear relation indicates that the BET surface area is consistent with the ECSA of FCMR (M=3, 10, 25, 40) electrocatalysts.

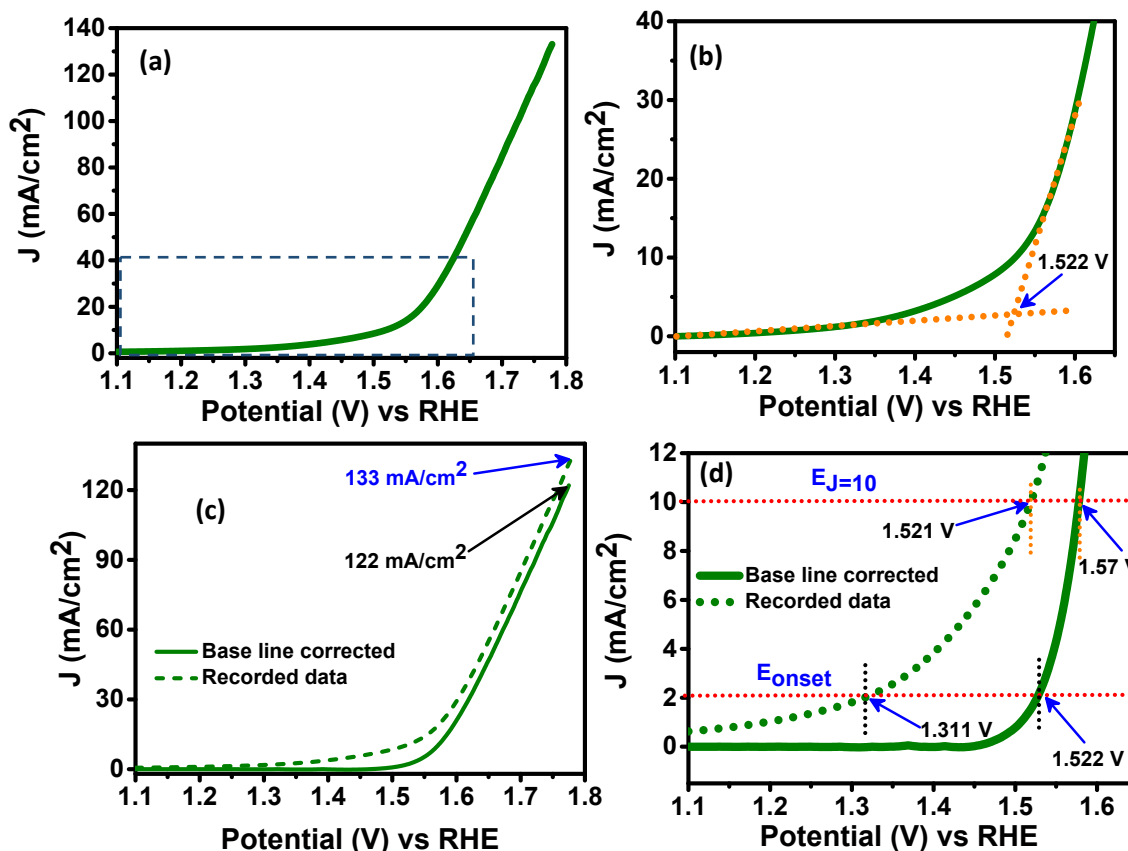


**Figure S5.** (a) As-recorded OER polarization curves on FC10R, (b) magnified portion of OER polarization curve marked in (a), (c) actual recorded and base line corrected OER polarization curve on FC10R. (d) magnified portion of OER polarization curves obtained from figure (c) for  $E_{\text{onset}}$  and  $E_{J=10}$  evaluation.

Figure S5a shows the OER polarization curve of FC10R recorded in nitrogen-saturated 1 M NaOH solution at 1200 rpm and 10 mV/s scan speed. A slow rising part is clearly observed below 1.5 V vs RHE which is clearly apparent in the magnified portion of OER polarization curve shown in figure S5b). In an attempt to minimize the contribution from various possible processes other than OER, the base line correction was carried out and Figure S5c shows the comparison of OER polarization curves before and after baseline correction. The onset potential which is taken as the  $E_{j=2 \text{ mA/cm}^2}$  is found to be 1.311 V before baseline correction and

is 1.522 V after the baseline correction. Similarly,  $E_{j=10}$  is found to be 1.57 V vs RHE after baseline correction as seen from Figure S5d. For more accurate determination of OER onset potential the two tangents are drawn as shown in figure b, they intersect at  $V = 1.522$  V, which is in agreement to the result obtained through RRDE set-up as shown in figure 4a,b (in main text).

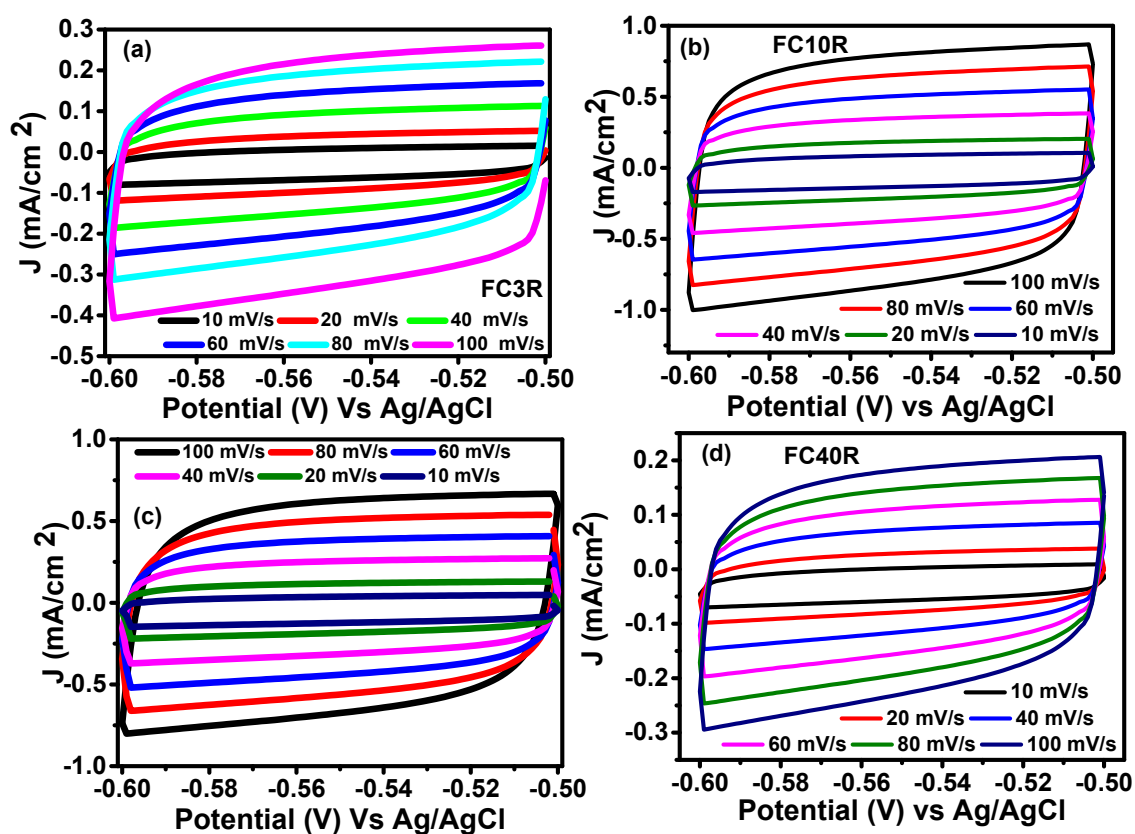


**Figure S6.** (a-d) Cyclic voltammograms on FCMR (M=3, 10, 25, 40) in 1 M NaOH nitrogen-purged aqueous solution at different scan rate in non-Faradic region in the potential window of -0.5 to -0.6 V vs Ag/AgCl (0.535 to 0.635 V vs RHE).



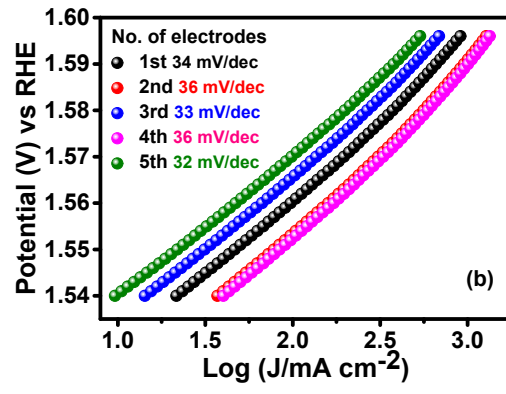
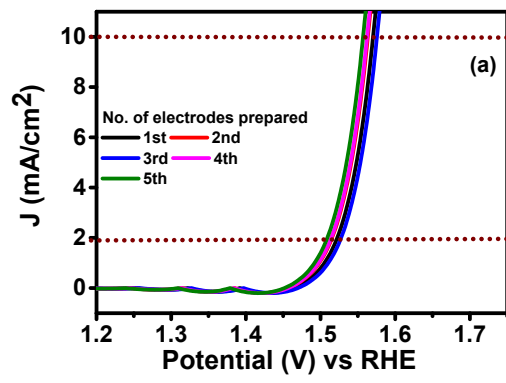


**Figure S7.** (a) RDE-LSV polarization curves, (b) corresponding Tafel slopes for OER on five different FC10R modified GCE in nitrogen-purged alkaline (1 M NaOH) solution with 10 mV/s scan speed and electrode rotation speed of 1200 rpm.

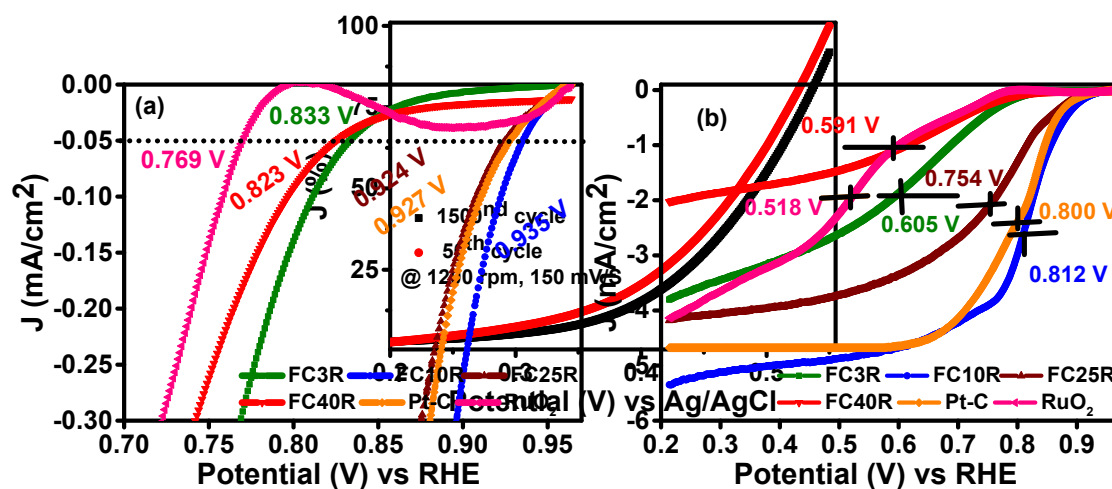


**Figure S8.** RDE-LSV polarization curves for OER corresponding to 50th and 1500nd cycles of accelerated stability test on FC10R in nitrogen-purged alkaline (1 M NaOH) solution with 100 mV/s scan speed and electrode rotation speed of 1200 rpm.

**Figure S9.** (a) Magnified portion of RDE-LSV polarization curves for onset potential and (b) for  $E_{1/2}$  determination for ORR in 0.1 M NaOH solution on  $\text{RuO}_2$ , Pt-C, FC3R, FC10R, FC25R and on FC40R. Here, the potential at which the ORR current density is  $0.05 \text{ mA/cm}^2$  is taken as onset potential.

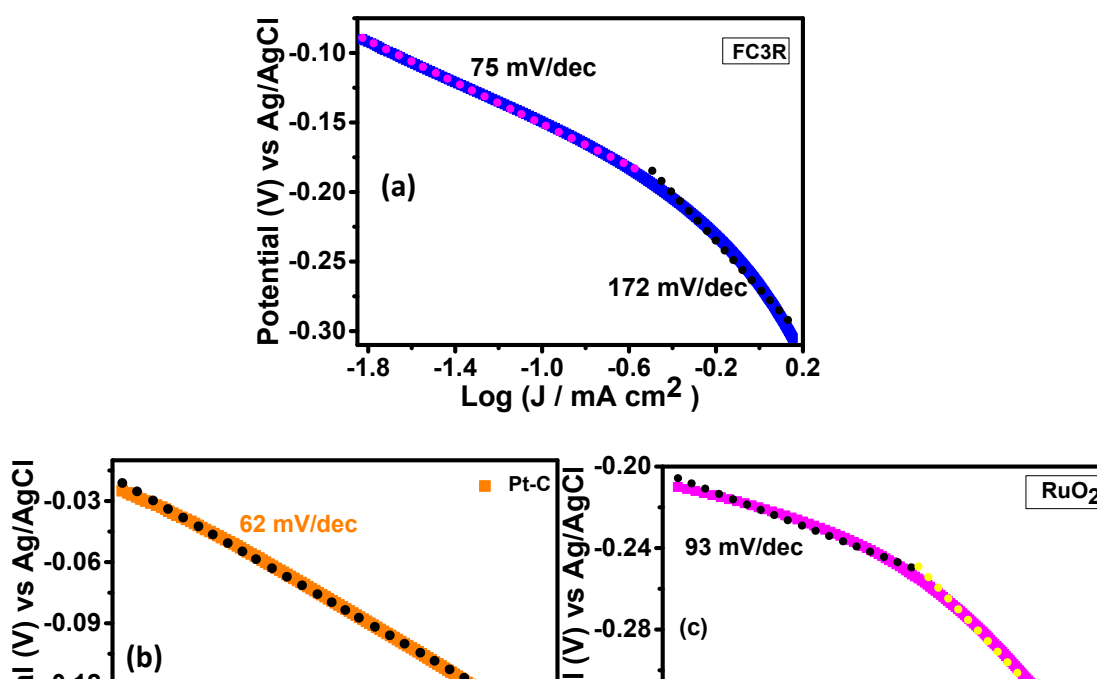


**Figure S10.** Tafel slope evaluation in low and high-over potential regions for (a) FC3R, (b) Pt-C, and (c) RuO<sub>2</sub>.

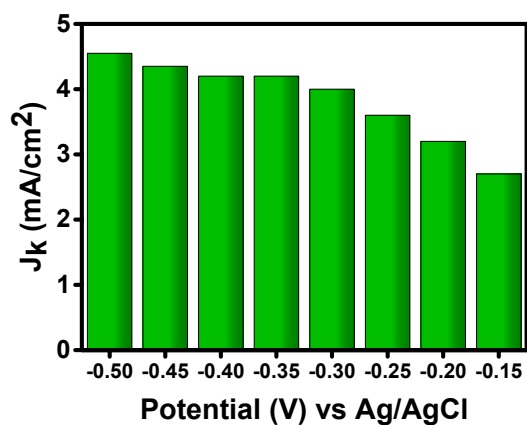


**Figure S11.** Normalized kinetic current density ( $J_k$ ) at different electrode potentials determined from the intercepts obtained from corresponding K-L plots analysis in mixed control region on FC10R.

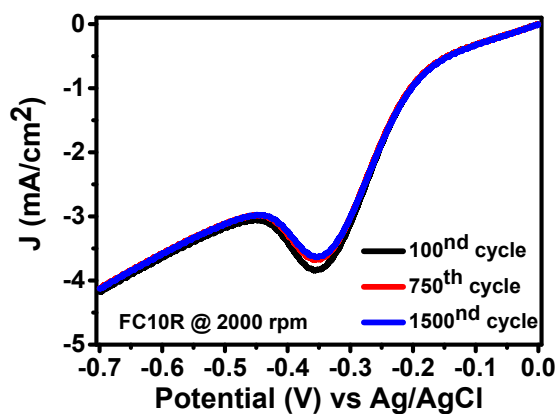


**Figure S12.** RDE-LSV polarization curves for ORR corresponding to 100<sup>th</sup>, 750<sup>th</sup> and 1500<sup>nd</sup> cycles of accelerated stability test on FC10R in oxygen-purged alkaline (0.1 M NaOH) solution with 100 mV/s scan speed and electrode rotation speed of 2000 rpm.

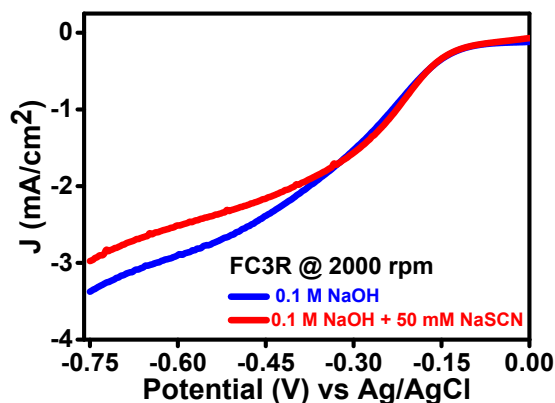


**Figure S13.** RRDE voltammograms recorded on FC3R in oxygen saturated 0.1 M NaOH and 0.1 M NaOH + 50 mM NaSCN medium at 2000 rpm electrode rotation and 10 mV/s scan speed.

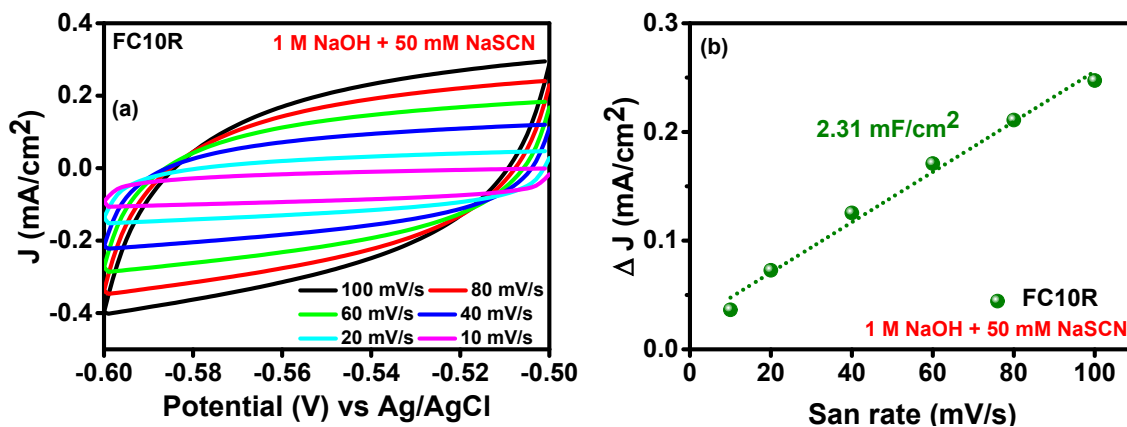


**Figure S14.** (a,b) Cyclic voltammograms on FC10R in 1 M NaOH + 50 mM NaSCN nitrogen-purged aqueous solution at different scan rate in non-Faradic region. (b) Double layer capacitance of FC10R deduced from cyclic voltammograms figure (a)

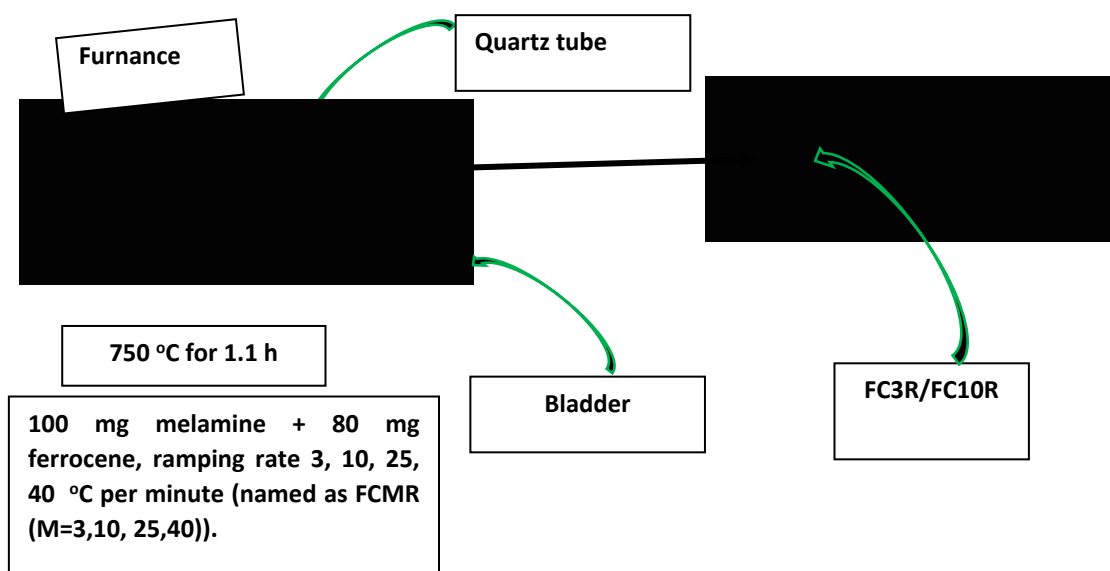


**Figure S15.** Schematic representation of synthesis procedure of FCMR (M= 3, 10, 25, 40). The quartz tube loaded with precursors and the close end was kept at the middle position of the furnace.

**Table S1.** Summarise the BET surface area for some carbon based oxygen electrocatalysts.

Catalyst	BET surface area	Reference
NiCo <sub>2</sub> O <sub>4</sub> /Graphene	77 m <sup>2</sup> g <sup>-1</sup>	<i>J. Mater. Chem. A</i> <b>2013</b> , <i>1</i> , 4754.
CoFe <sub>2</sub> O <sub>4</sub> /N-P-biocarbon	79.84 m <sup>2</sup> g <sup>-1</sup>	<i>J. Mater. Chem. A</i> <b>2014</b> , <i>2</i> , 18012.
MWCNT@S-N-C	121 m <sup>2</sup> g <sup>-1</sup>	<i>New J. Chem.</i> <b>2015</b> , <i>39</i> , 6289.

CoFe <sub>2</sub> O <sub>4</sub> /rGO	173.12 m <sup>2</sup> g <sup>-1</sup>	<i>Journal of Power Sources</i> <b>2014</b> , 250, 196.
Fe/Fe <sub>3</sub> C@NGL-NCNT	210 m <sup>2</sup> g <sup>-1</sup>	<i>Chem. Commun.</i> <b>2015</b> , 51, 2710.
FC3R	92 m <sup>2</sup> g <sup>-1</sup>	Present study
<b>FC10R</b>	<b>240 m<sup>2</sup>g<sup>-1</sup></b>	<b>Present study</b>

**Table S2.** OER activity summary for various carbon-based electrocatalyst.

Electrocatalyst	Experimental Medium and loading of electrocatalyst	$E_{\text{on-set}}$ (mV) Vs Ag/AgCl	$E_{J=10}$ (mV) Vs Ag/AgCl	Reference
CoFe <sub>2</sub> O <sub>4</sub> /rGO	0.1 M KOH, 1.006 mg/cm <sup>2</sup>	540	700	Journal of Power Sources 250 (2014) 196e203
FeCo <sub>2</sub> O <sub>4</sub> -HrGOS	0.1 M KOH, 1.006 mg/cm <sup>2</sup>	570	750	Carbon 92 (2015) 74–83
CoFe <sub>2</sub> O <sub>4</sub> /CNTs	0.1 M KOH, 1.006 mg/cm <sup>2</sup>	600	700	Electrochimica Acta 177 (2015) 65–72
MWCNT@S–N–C	0.1 M KOH, 0.200 mg/cm <sup>2</sup>	600	700	<i>New J. Chem.</i> , 2015, 39, 6289--6296
S,N,Fe-porous carbon	0.1 M KOH, 0.100 mg/cm <sup>2</sup>	----	650	<i>Green Chem.</i> , 2016, <b>18</b> , 4004-4011
N-doped Fe-Fe <sub>3</sub> C@ graphitic layer	0.1 M KOH, 0.710 mg/cm <sup>2</sup>	600	778	Green Chemistry 18 (2016), 427-432
Nitrogen-doped Fe/Fe <sub>3</sub> C@graphitic layer/carbon nanotube	0.1 M KOH 0.103 mg/cm <sup>2</sup>	500	850	<i>Chem. Commun.</i> , 2015, <b>51</b> , 2710-2713
NiCo <sub>2</sub> S <sub>4</sub> @N/SrGO	0.1 M KOH 0.283 mg/cm <sup>2</sup>	600	720	<i>ACS Appl. Mater. Interfaces</i> , 2013, 5 (11), pp 5002–5008
BFNCNTs	1 M NaOH 0.75 mg/cm <sup>2</sup>	422	562	J. Mater. Chem. A, (2017), DOI: 10.1039/c7ta04597b
FC3R	1 M NaOH 1 mg/cm <sup>2</sup>	620	705	Present work
<b>FC10R</b>	<b>1 M NaOH 1 mg/cm<sup>2</sup></b>	<b>380</b>	<b>550</b>	<b>Present work</b>

**Table S3.** ORR activity summary for various carbon-based electrocatalyst.

Electrocatalyst	Experimental Medium and loading of electrocatalyst	E <sub>on-set</sub> (mV) Vs (Ag/AgCl)	E <sub>1/2</sub> (Vs Ag/AgCl)	Reference
MWCNT@S-N-C	0.1 M KOH, 0.2 mg/cm <sup>2</sup>	-200	~-350	<i>New J. Chem.</i> , 2015, 39, 6289--6296
CoFe <sub>2</sub> O <sub>4</sub> /CNTs	0.1 M KOH, 1.006 mg/cm <sup>2</sup>	-124	~-300	<i>Electrochimica Acta</i> 177 (2015) 65–72
CoFe <sub>2</sub> O <sub>4</sub> /rGO	0.1 M KOH, 1.006 mg/cm <sup>2</sup>	-136	~-260	<i>Journal of Power Sources</i> 250 (2014) 196e203
Co-N-GN	0.1 M KOH, 0.1 mg/cm <sup>2</sup>	-98	-162	<i>J. Mater. Chem. A</i> , 2013, 1, 3593-3599
N,P,S-rGO/ <i>E. coli</i>	0.1 M KOH, 0.510 mg/cm <sup>2</sup>	-90	~-220	<i>J. Mater. Chem. A</i> 2015,3, 12873-12879
FeCo <sub>2</sub> O <sub>4</sub> -HrGOS	0.1 M KOH, 1.006 mg/cm <sup>2</sup>	-90	~-200	<i>CARBON</i> 92 ( 2015 ) 74 –83
N-graphene/CNT hybrids	0.1 M KOH, 0.430 mg/cm <sup>2</sup>	-80	~-200	<i>Angew. Chem. Int. Ed.</i> 2014, 53, 6496 - 6500
N-CNTs	0.1 M KOH, 0.306 mg/cm <sup>2</sup>	-60	-220	<i>Carbon</i> 50 ( 2012 ) 2620-2627
N,S-Graphene	0.1 M KOH, 0.43 mg/cm <sup>2</sup>	-60	-300	<i>Angew. Chem., Int. Ed.</i> , 2012, 51, 11496
BFNCNTs	0.1 M NaOH 0.75 mg/cm <sup>2</sup>	-30	-225	<i>J. Mater. Chem. A</i> , (2017), DOI: 10.1039/c7ta04597b
FC3R	0.1 M NaOH 1 mg/cm <sup>2</sup>	-125	-330	Present work
<b>FC10R</b>	<b>0.1 M NaOH 1 mg/cm<sup>2</sup></b>	<b>-25</b>	<b>-155</b>	<b>Present work</b>

**Table S4.** Overall oxygen electroactivity ( $\Delta E$ ) summary for various carbon-based electrocatalyst.

Catalyst	Overall oxygen electrode activity $\Delta E (E_{j=10(\text{OER})} - E_{1/2(\text{ORR})})(\text{V})$	Reference
S-N-C@MWNCNTs	~1.25	<i>New J. Chem.</i> 2015, 39, 6289.
NCNF-1000	~1.02	<i>Adv. Mater.</i> 2016, 28, 3000–3006.
Fe/Fe <sub>3</sub> C@NGL-NCNT	~1	<i>Chem. Commun.</i> 2015, 51, 2710.
N-Graphene/CNTs	~1.00	<i>Small</i> , 2014, 10, 2251.
B-MWNCNTs	~1.00	<i>Electrochimica Acta</i> 2014,143, 291.
CoFe <sub>2</sub> O <sub>4</sub> /rGO	~0.98	<i>J. Power Sources</i> 2014, 250, 196.
CoFe <sub>2</sub> O <sub>4</sub> /N-P-biocarbon	~0.98	<i>J. Mater. Chem. A</i> 2014,2,18012.
N,P-Carbon paper	~ 0.96	<i>Angew. Chem. Int. Ed.</i> 2015, 54, 4646.
P-doped g-C <sub>3</sub> N <sub>4</sub> /CF	~0.96	<i>Angew. Chem. Int. Ed.</i> 2015, 54, 4646–4650.
Fe/Fe <sub>3</sub> C@ N-graphitic layer	~ 0.97	<i>Green Chemistry</i> 2015, DOI: 10.1039/c5gc01405k
Pt@C	~0.94	<i>Angew. Chem. Int. Ed.</i> 2014, 53, 8508.
Mn <sub>2</sub> O <sub>3</sub> /N-Carbon	~0.93	<i>Angew. Chem. Int. Ed.</i> 2014, 53, 8508.
Ir@C	~0.92	<i>J. Am. Chem. Soc.</i> 2010,132, 3612.
NiCo <sub>2</sub> O <sub>4</sub> /Graphene	~0.915	<i>J. Mater. Chem. A</i> 2013,1,4754.
N, S, O carbon nanosheet	~0.88	<i>Nano Energy</i> 19 (2016) 373–381
Fe@N-C	~0.88	<i>Nano Energy</i> 2015, 13, 387–396.
NiO/CoN PINWs	~0.8	<i>ACS Nano</i> , 2017, 11 (2), pp 2275–2283
Fe/N/C@BMZIF	~0.79	<i>ACS Appl. Mater. Interfaces</i> , 2017, 9 (6), pp 5213–5221
BFNCNTs	~0.788	<i>J. Mater. Chem. A</i> , (2017), DOI: 10.1039/c7ta04597b
FC3R	~1.035	Present work
<b>FC10R</b>	~0.758	<b>Present work</b>